PHILOSOPHICAL TRANSACTIONS OF THE ROYAL SOCIETY A MATHEMATICAL, PHYSICAL & ENGINEERING SCIENCES

The Influence of Convection on the Structure of the High-Latitude Ionosphere [and Discussion]

S. Quegan, A. S. Rodger, P. J. S. Williams, M. Lockwood and H. Rishbeth

Phil. Trans. R. Soc. Lond. A 1989 **328**, 119-137
doi: 10.1098/rsta.1989.0028

Phil. Trans. R. Soc. Lond. A **328**, 119–137 (1989)
Printed in Great Britain

The influence of convection on the structure of the high-latitude ionosphere

By S. Quegan

Department of Applied and Computational Mathematics, University of Sheffield, Sheffield S10 2TN, U.K.

[Plates 1 and 2]

Fundamental to the understanding of high-latitude ionospheric behaviour is an appreciation of the convection electric field and its consequences. This electric field drives a number of processes which directly influence the plasma, including vertical ion drifts, Joule heating and enhanced neutral air velocities. Particle precipitation regions are closely connected with convection boundaries. Universal time variations can, in many cases, be directly related to the diurnal variation of the convection electric field in the geographical frame. Convection also has a profound influence on the interpretation of observations, because understanding why plasma densities have their observed characteristics requires knowledge of the past history of the observed plasma. This past history is determined by the convection electric field, as it transports plasma between regions of differing dominant plasma processes. Where reasonable estimates of the convection electric field exist, numerical models of the ionosphere seem capable of reproducing the characteristics of observed plasma behaviour. This is demonstrated by using the European incoherent-scatter facility's observations for days for which such estimates are available.

1. Introduction

When we observe ionospheric plasma, we observe a system with a memory. The plasma we see carries the imprint of its history with it. The duration of ionospheric memory is dependent on the timescales of the dominant processes affecting the plasma. Hence, understanding observations implies that we need to know the history of the plasma on the timescales of the dominant processes. At mid-latitudes, the history of the observed plasma is to a large extent predictable, because the horizontal transport of plasma is due to corotation. Night follows day in an orderly fashion; neighbouring parcels of plasma have similar histories. At high latitudes, the situation is quite different, as illustrated by figure 1 (from Quegan *et al.* 1982), which shows a snapshot of an idealized convection pattern due to Heelis *et al.* (1982). An obvious characteristic of this convection pattern is the great variety of convection paths within it; plasma on path number 5 suffers a reversal of flow direction in the dusk sector, and takes many hours to perform a full convection cycle; plasma on path number 2 spends many hours near one (magnetic) position in the polar cap; plasma on path number 1 performs its cycle in less than five hours. Note also that near neighbours can have quite different histories (compare paths 1 and 2 near 70° magnitude latitude on the dawn meridian, or paths 5 and 7 in the dusk sector). The history of the plasma is no longer readily predictable at high latitudes; no longer do neighbouring parcels of plasma have the same history.

To understand the effects of these different histories, we must take account of where the

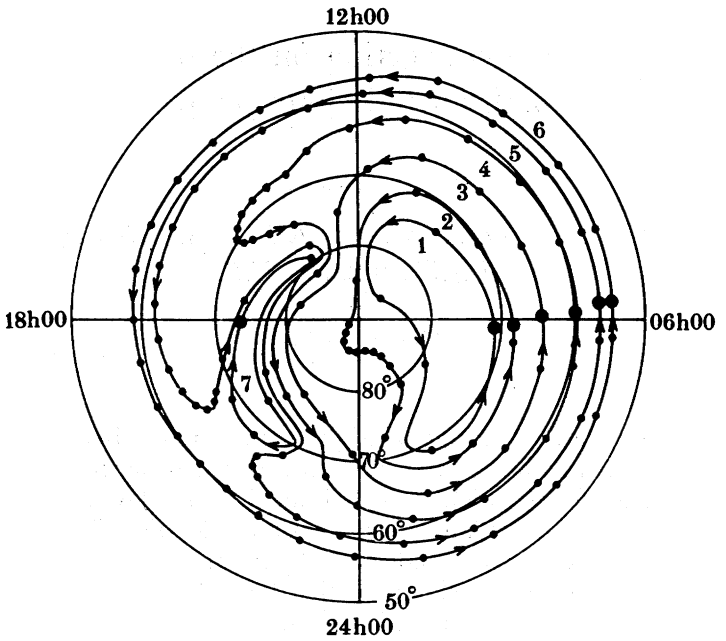

FIGURE 1. Representation in the non-corotating geomagnetic frame of a convection pattern due to Heelis *et al.* (1982). Successive marks on the figure show a convection time of 1 h, starting points being indicated by the large solid circles. Circles (crosses) indicate a solar zenith angle less than (greater than) 104°, for a solar declination of −23.5°. The numbers on the paths correspond to the path potentials. The key is as follows: 1, 7.0 kV; 2, −0.5 kV; 3, −9.5 kV; 4, −17.0 kV; 5, −22.5 kV; 6, −25.5 kV; 7, −24.55 kV.

plasma has been over the preceding hours, and the processes to which it has been subjected on its travels. A fundamental determinant of the transport is the magnetospheric electric field $\boldsymbol{E}_{\mathrm{m}}$ and the associated plasma convection velocity perpendicular to the magnetic field

$$\boldsymbol{v}_{\perp} = \boldsymbol{E}_{\mathrm{m}} \times \boldsymbol{B}/B^2, \tag{1}$$

where $\boldsymbol{B}$ is the magnetic field. An obvious effect of convection is to transport plasma between regions of differing dominant processes. A full appreciation of the effects of convection, however, requires us to understand how deeply embedded convection is in causing or modifying these processes.

In this paper we aim to show how intimately the structure of the high-latitude ionosphere is related to plasma convection, and how a proper understanding of high-latitude phenomena must take into account both very obvious and very subtle effects of convection. The first part of the paper deals with the processes which determine high-latitude ionospheric plasma densities, and discusses the relation of each process to plasma convection. While the first part will give numerous examples of high-latitude structures and observations related to convection, in the second part of the paper we describe two highly contrasting situations where plasma convection is central to understanding the observations. In the concluding remarks we will note a number of open questions relating to convection and its ionospheric effects.

PHILOSOPHICAL TRANSACTIONS OF THE ROYAL SOCIETY A MATHEMATICAL, PHYSICAL & ENGINEERING SCIENCES

2. Plasma processes

The high-latitude ionosphere is affected by a large number of processes, which interact in complex ways, and which are all connected with convection in some way. In this section we examine these processes and connections. The processes which we consider are

(*a*) plasma transport;
(*b*) photoionization;
(*c*) ion chemistry;
(*d*) particle precipitation;
(*e*) ionosphere–thermosphere interactions;
(*f*) ionospheric or magnetospheric field-aligned flow;
(*g*) Universal Time (U.T.) variations.

This is not meant to be an exhaustive list of processes connected with convection. In particular, wave–particle interactions and plasma instabilities are not discussed here, even though they are certainly related to convection and convection boundaries (see, for example, Moore *et al.* 1986; Rino & Vickrey 1982). However, the processes listed above are the main determinants of the large-scale structure of the high-latitude ionosphere.

2.1. *Plasma transport*

The most obvious example of plasma transport at high latitudes is plasma convection itself, as described by (1), but a full appreciation of plasma transport needs to take into consideration its three-dimensional nature. Above *ca.* 180 km, plasma motions can apparently be dynamically decoupled into field-perpendicular (convective) and field-aligned (diffusive) motions (Schunk 1975). However, because of the coupling of the ion and neutral gases, the convective motion creates a number of effects which feed into diffusion; we shall consider these effects after discussing convection itself.

Ionospheric convection is driven by the interaction of the solar wind with the Earth's magnetic field. Our understanding of the mechanisms and ionospheric signatures of this interaction is developing rapidly. Connection of interplanetary magnetic field (IMF) lines with the Earth's magnetic field (Dungey 1961) is thought to provide the major proportion of the electric potential difference driving convection, with viscous interactions providing a small but measureable proportion of the total cross-tail potential difference (Hill 1983; Reiff *et al.* 1981; Mozer 1984). The orientation of the IMF is known to have profound effects on the nature of the convection. The most marked effects occur when the north–south component of the IMF (B_z) has different signs. For B_z negative, a characteristic two-celled pattern is expected (Heelis & Reiff 1985; Heppner & Maynard 1983, 1987), with antisunward motion over the polar cap and return flow round the flanks (see figure 2). For B_z positive, multicelled convection patterns seem possible, with sunward flow at high latitudes (Rezhenov 1981; Reiff 1982; Zanetti *et al.* 1984); there is still discussion as to whether measurements confirm these multicelled structures, the major dissenting voices being Heppner & Maynard (1983, 1987) who consider that observations may instead correspond to distorted two-celled patterns.

The sign of B_y is also known to significantly affect the electric potential distribution at high latitudes (Cowley 1981*a*, and references). Figure 2, taken from Heppner & Maynard (1987) makes these differences clear. In the Northern Hemisphere electric fields tend to be higher on the dusk side of the polar cap when B_y is negative and higher on the dawn side when B_y is

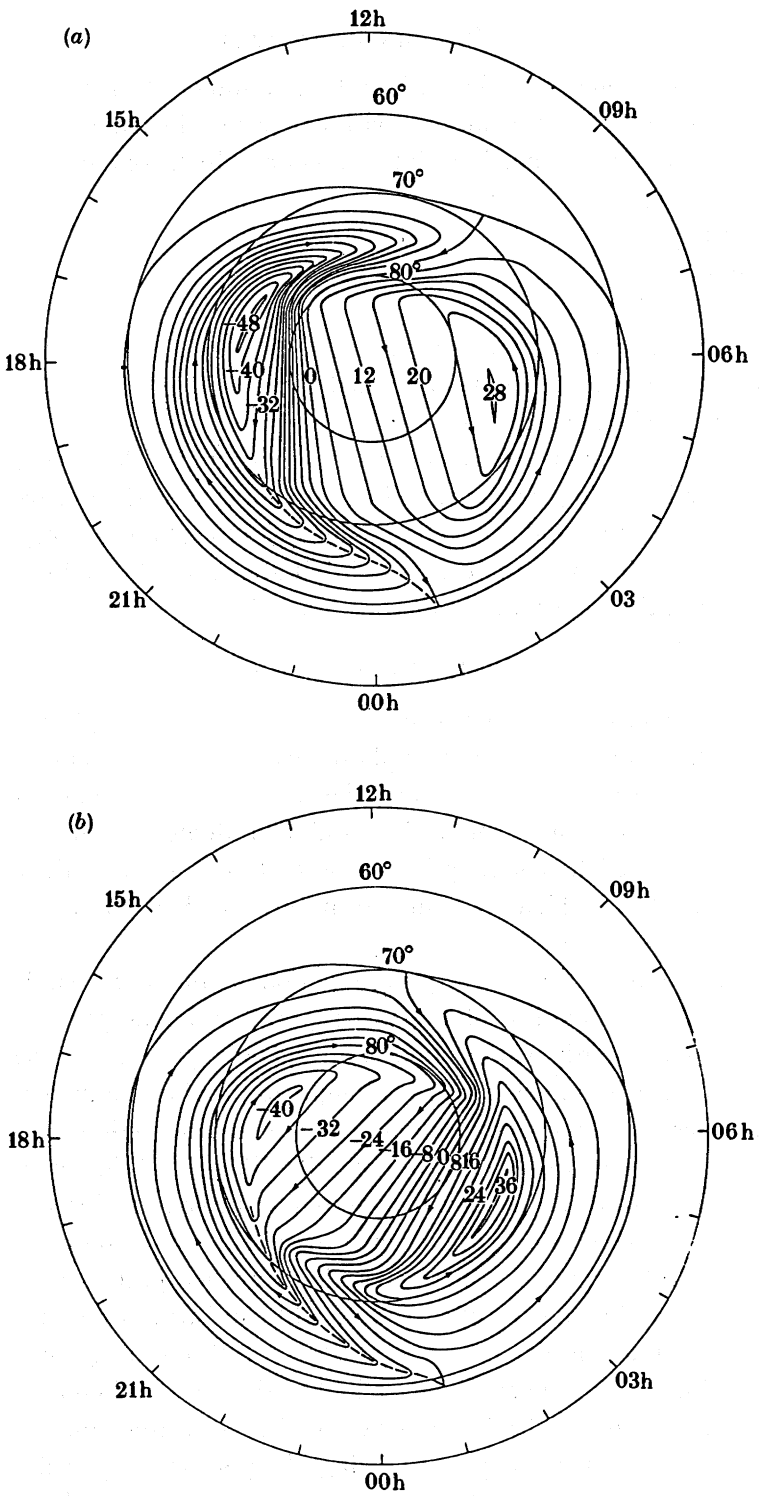

FIGURE 2. Model electric potential distributions due to Heppner & Maynard (1987). In the Northern Hemisphere, (*a*) (model BC) is appropriate for B_y negative and (*b*) (model DE) is appropriate for B_y positive; this correspondence is reversed in the Southern Hemisphere.

positive this situation is reversed in the Southern Hemisphere. These asymmetries in the potential distribution lead to marked effects in the observed convective flows. As an example, the potential distribution for positive B_y causes a region of slow flow in the northern dusk side polar cap. Figure 3, plate 1, shows the European incoherent scatter facility's (EISCAT's) data from the Polar special programme for 25 October 1984 for a time of comparatively steady positive B_y and negative B_z conditions. A region of slow flow near 17h00 magnetic local time (MLT) mean local time on the dusk side is quite clear, as are such features as an entry region into the polar cap in the pre-noon sector, and strong westward flows associated with the dusk cell. The morning cell leaves no obvious signature in the data.

An essential element in attempting to describe the effects of convection quantitatively is a description of the electric field distribution at high latitudes. Important contributions to this end have been made by Volland (1975), Heppner (1977), Heppner & Maynard (1983, 1987) and Heelis *et al.* (1982), who have produced tabulated or analytic models of electric field distributions corresponding to differing conditions. Several studies have attempted to compare these model descriptions with observations (Sojka *et al.* 1980; Sojka & Schunk 1986; Quegan *et al.* 1988). As an example, many of the features of the convection data shown in figure 3 can be reproduced by the Heppner model for B_y positive (figure 2*b*), as figure 4 illustrates.

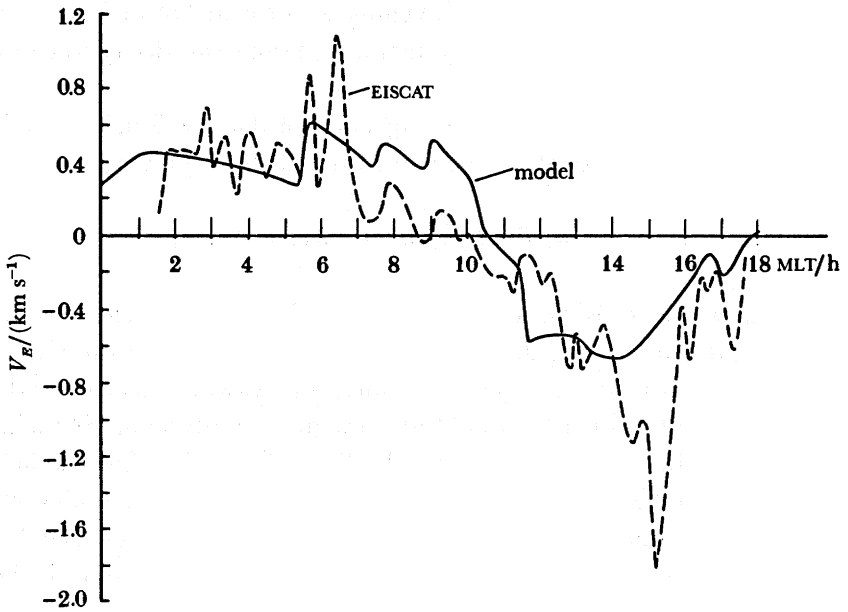

FIGURE 4. Observed and calculated eastward velocities corresponding to gate 3 of the observations shown in figure 3. The observed velocities shown are 12½ min averages. The calculated velocities are derived from the electric potential distribution shown in figure 2 (*b*), displaced 4° towards dusk and 4° towards noon in the invariant-latitude–MLT frame.

Figure 4 is a comparison between the zonal component of the $E \times B$ drift measured by EISCAT at gate 3 (at an altitude of *ca.* 277 km) for this data shown in figure 3, and values calculated using the Heppner & Maynard model appropriate to these conditions (figure 2*b*). There is reasonable agreement between the model and the observations. The phasing of the change from eastward to westward flow is approximately correct, and the calculated velocities are also approximately correct (including the marked drop in velocities near dusk) except for the region

of rapid flow observed in the afternoon, which is not reproduced by the model electric field. To obtain this agreement, the Heppner & Maynard model was displaced 4° towards dusk and 4° towards noon, but no other changes were made. No analysis of the best displacement needed to match the observations was made; a fuller discussion of this point will be found in Quegan *et al.* (1988).

The B_x component of the IMF is also expected to affect polar cap structure, but not as significantly as the B_y and B_z components (Cowley 1981*b*; Heppner & Maynard 1987).

The equipotential distributions shown in figure 2 do not include the effects of corotation, and indicate the flow directions and velocities expected to be observed from a station corotating with the Earth, such as EISCAT. When we convert to a non-rotating frame (which is more suitable for satellite observations) we can regard the total electric field, $\boldsymbol{E}$, as the sum of a convection electric field ($\boldsymbol{E}_{\mathrm{m}}$) and a corotation electric field ($\boldsymbol{E}_{\mathrm{c}}$)

$$\boldsymbol{E} = \boldsymbol{E}_{\mathrm{m}} + \boldsymbol{E}_{\mathrm{c}}. \tag{2}$$

This combined field gives rise to plasma trajectories showing great variation in behaviour and in the time taken to perform a full convection cycle. We have already noted such effects when discussing figure 1, which shows the convection pattern in a non-corotating frame. In this frame, those regions where convection and corotation compete and cause plasma to become nearly stationary are made obvious (e.g. the evening sector near 65° in figure 1); such regions are important because, in the absence of production, plasma can decay to cause ionospheric troughs and holes.

Figures 1 and 2 show only the horizontal projection of the $\boldsymbol{E}\times\boldsymbol{B}$ drift. Important also for ionospheric behaviour is the vertical component of this drift, of magnitude

$$v_z = (E_\phi/B)\sin\theta/(1+3\cos^2\theta)^{\frac{1}{2}}, \tag{3}$$

where v_z is positive upwards, E_ϕ is the zonal component of the electric field (positive eastwards), B is the magnitude of the magnetic field, and θ is magnetic colatitude, assuming a dipolar form for the magnetic field. This drift can be significant; an eastward electric field of 1 mV m^{-1} represents an upward drift of *ca.* 1 km min^{-1} at a magnetic latitude of 70°; a westward field produces a downward drift of the same magnitude. For a dawn–dusk electric field this implies that drifts are upwards on the dayside and downwards on the nightside. Such vertical drifts can have drastic effects on plasma densities because they drive plasma to regions of higher or lower neutral gas concentrations, and hence to regions of enhanced or reduced chemical decay rates.

Proper analysis of the effects of these vertical electrodynamic drifts is not straightforward, however, because plasma transport in the vertical direction must also take into account field-aligned diffusion. In its simplest form, the field-aligned momentum equation for the ion i in an ion/neutral gas mixture is given by

$$v_{\mathrm{i}}'' = v_{\mathrm{n}}'' - k\left[(T/n_{\mathrm{i}})\nabla'' n_{\mathrm{i}} - \frac{m_{\mathrm{i}} G''}{k} + \nabla'' T\right] \Big/ (m_{\mathrm{i}}\nu_{\mathrm{in}}), \tag{4}$$

where

v_{i}'' is the field-aligned component of the ion velocity;

v_{n}'' is the field-aligned component of the neutral gas velocity;

PHILOSOPHICAL TRANSACTIONS OF THE ROYAL SOCIETY A MATHEMATICAL, PHYSICAL & ENGINEERING SCIENCES

k is the Boltzmann's constant;
m_i is the ion mass;
ν_{in} is the ion–neutral collision frequency;
$T = T_e + T_i$ is the sum of electron and ion temperatures;
∇'' is the directional derivative along the magnetic field;
G'' is the field-aligned component of gravity.

The role of convection in this equation is not obvious, but is embedded in three terms, the temperature T, the collision frequency ν_{in} and the neutral gas velocity v_n''. Convection affects the first of these, because relative motion of the ions and neutrals leads to collisional heating (Joule heating) and enhanced T_i. This in turn acts to increase ν_{in}. The neutral gas velocity v_n'' is also markedly affected by convection, because at high latitudes ion drag provides a major source of momentum for the neutral gas. There are quite different timescales for these effects. For collisional heating, the timescale is of the order of seconds. Ion-drag acceleration of the neutral gas has widely varying timescales, dependent on the electron density, but is typically on the order of 1 h or greater. For periods of steady convection, the neutral gas is thus able to respond to convection, giving a reduced ion–neutral velocity and little collisional heating. During periods of changing electric fields, however, the neutral gas cannot respond immediately to such changes, leading to enhanced Joule heating.

Note that the dynamic coupling of the ions to the neutral gas tends to produce field-aligned ion drifts which oppose the $\boldsymbol{E} \times \boldsymbol{B}$ vertical drifts described above. The convection-driven flow of neutral gases from dayside to nightside at high latitudes tends to drive plasma to lower altitudes on the dayside and to higher altitudes on the nightside. As a result, simple treatments of how convection affects diffusion must be viewed with caution, particularly under time-varying conditions.

2.2. *Photoionization*

Figures 1 and 2 show convection patterns in the magnetic frame, but a proper appreciation of the consequences of convection must also consider the geographic frame. As an illustration, in figure 5 we show the same convection path in the magnetic (figure 5*a*) and geographic (figure 5*b*) frames. In figure 5*b* it is clear which parts of the plasma trajectories are in darkness (the solar terminator, indicating where the atmosphere below 120 km is in shadow, is marked by the solid line) and hence where chemical recombination can cause plasma to decay, yielding troughs. Note that following the convection reversal, marked [1], plasma does not return to sunlight until it arrives in the dawn sector, while following the convection reversal, marked [3], during a second traversal of the convection cycle, plasma returns to sunlight in the dusk sector. However, in both cases exposure to particle precipitation will occur near magnetic noon (at the foot of the cusp). This illustrates that only by considering convection in both frames can a proper reconstruction of the plasma history at any point be made.

2.3. *Ion chemistry*

The ion chemistry is affected by convection through the energy dependence of the two key reactions

$$O^+ + N_2 \xrightarrow{k_1} NO^+ + N, \tag{5}$$

$$O^+ + O_2 \xrightarrow{k_2} O_2^+ + O, \tag{6}$$

PHILOSOPHICAL TRANSACTIONS OF THE ROYAL SOCIETY A MATHEMATICAL, PHYSICAL & ENGINEERING SCIENCES

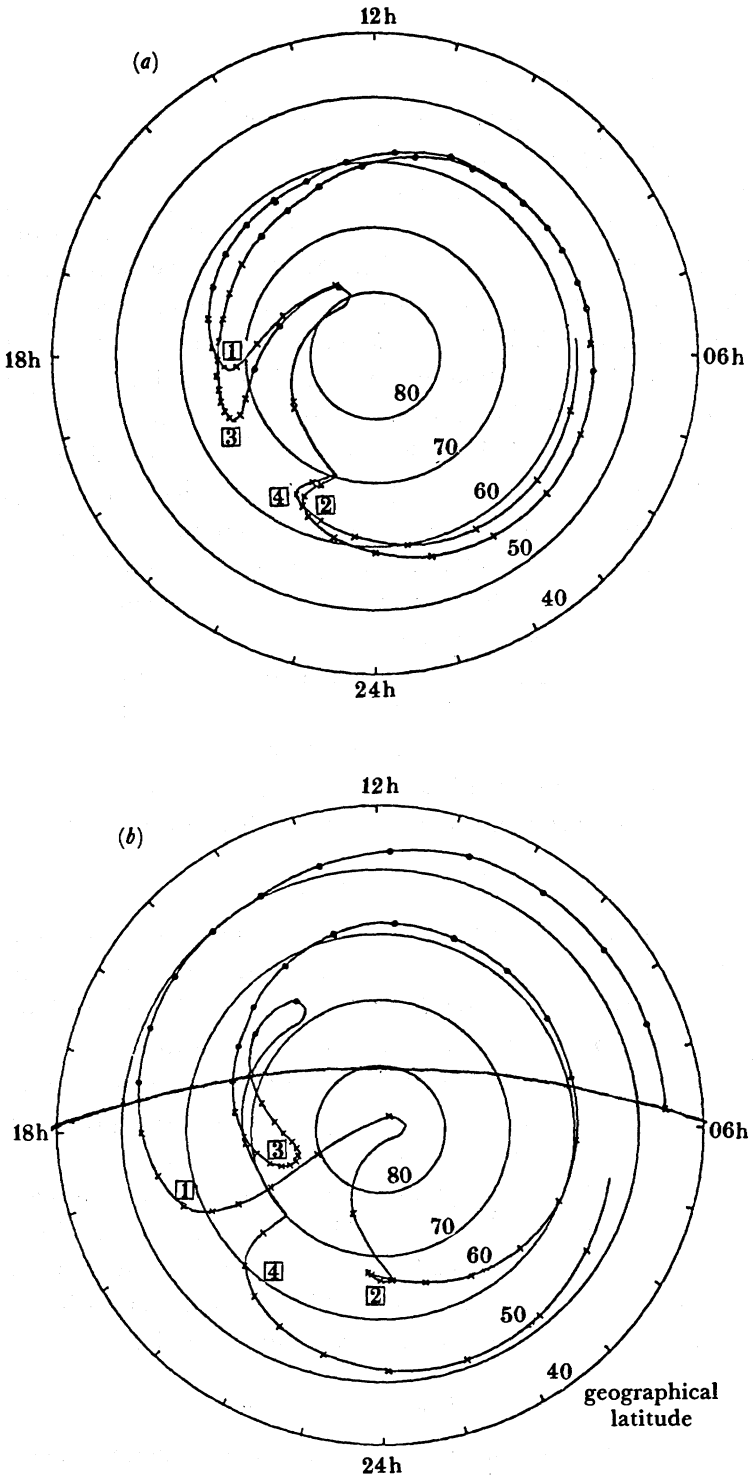

FIGURE 5. (*a*) Representation in the geomagnetic frame (magnetic local time/invariant latitude) and (*b*) geographic frame (solar local time/geographical latitude) of a convection path derived from a model electric field due to Heelis *et al.* (1982). Successive marks on a path indicate 1 h of travel time; circles (crosses) correspond to a solar zenith angle less than (greater than) 104°. The solar terminator is marked on (*b*). The boxed numbers indicate regions of slow flow in the magnetic frame.

which provide the major loss processes for O^+, and in combination with the much faster reactions

$$NO^+ + e^- \rightarrow N + O, \tag{7}$$

$$O_2^+ + e^- \rightarrow O + O, \tag{8}$$

the major loss processes for free electrons. The energy-dependence of these reactions was derived in terms of fitted polynomials of an effective temperature T_{eff} by St Maurice & Torr (1978), where

$$T_{\text{eff}} = T_n + m_n|\boldsymbol{v}_i - \boldsymbol{v}_n|^2/3k. \tag{9}$$

Here T_n and m_n are the neutral gas temperature and mass, respectively, $\boldsymbol{v}_i$ and $\boldsymbol{v}_n$ are the ion and neutral bulk velocities, k is Boltzmann's constant, and we have assumed that the ions and neutral species are in thermal equilibrium (this assumption causes T_{eff} to be underestimated because it ignores thermal coupling to the electrons; however, this does not affect the importance of the relative drift term and the discussion below). The influence of convection is given directly by the term in $|\boldsymbol{v}_i - \boldsymbol{v}_n|^2$.

The behaviour of k_1 and k_2 is discussed by St Maurice & Torr (1978); in each case, as the ion–neutral relative velocity increases, both k_1 and k_2 initially decrease; it is not until $T_{\text{eff}} \gtrsim 1800$ K that the decay rate by reaction (5) (which is most important for F-layer electron densities) becomes enhanced.

The enhanced decay rate associated with fast convection has been cited by numerous authors as a mechanism for the formation of both high-latitude troughs and the mid-latitude trough (see, for example, Pinnock 1985; Grebowsky *et al.* 1983; Evans *et al.* 1983), because regions of anomalously high NO^+ concentrations are often found in association with regions of fast convection and ionospheric electron density troughs. However, no convincing quantitative study of this hypothesis has yet been published, largely because of the difficulty of producing a consistent set of input conditions on which to base the calculations. The difficulty in invoking convection-induced enhancement in the plasma decay rate as a trough formation mechanism is that the same convection is transporting the plasma large distances while it decays, and slower-moving plasma in the same region will have had longer to decay. The following example illustrates this point, while not purporting to be a realistic model of circumstances occurring at high latitudes (as already pointed out, such a realistic model is not available).

We assume a corotating neutral atmosphere at a temperature of 1000 K and consider two neighbouring parcels of plasma at 20° colatitude which at time 0 have the same density and are on the solar terminator. At this time one of the parcels is subjected to an enhanced velocity of 2 km s^{-1} in the eastward direction compared to its corotating neighbour. As a result k_1 increases from 5.3×10^{-19} to *ca.* 1.0×10^{-17} m^3 s^{-1}. However, the important parameter is k_1/U, where U is the ion–neutral relative speed. Larger values of this parameter imply lower densities. For the fast-moving plasma, this parameter has a value 4.7×10^{-21} m^2, while for plasma which is corotating this parameter has the value 3.2×10^{-21} m. Hence the velocity enhancement will cause the plasma in the fast-moving jet to have lower densities than neighbouring corotating plasma. A factor e depletion would be produced *ca.* 1100 km into the nightside. To obtain this depletion, the velocity must be enhanced for the whole period of travel and the neutral atmosphere must not respond to the convection and reduce the ion–neutral relative velocity. Note that large velocity enhancements are required; for the conditions of the example, velocities less than 1.7 km s^{-1} would have caused the fast-moving jet to be a region of *enhanced* densities.

PHILOSOPHICAL TRANSACTIONS OF THE ROYAL SOCIETY A MATHEMATICAL, PHYSICAL & ENGINEERING SCIENCES

2.4. *Particle precipitation*

Convection and precipitation are intimately linked, both empirically and theoretically (Heelis *et al.* 1980). However, there does not exist at the moment any link strong enough to enable quantitative prediction of precipitation boundaries and characteristics from a given convection pattern, nor is there any satisfactory description of how, after reconnection in a largely homogeneous plasma sheet, flux tubes produce differing quantities of precipitation, leading to spatial and temporal variation in observed precipitation. Descriptions of precipitation in the form of statistical models carry only a weak link with convection in terms of an activity level (Spiro *et al.* 1982; Fuller-Rowell & Evans 1987). Another inadequacy in the precipitation models is that, because of averaging, sharp boundaries have been lost, even though such boundaries are clearly present in observations of precipitation (Rodger *et al.* 1986; Heelis *et al.* 1980). By contrast, convection models (see, for example, Heppner 1977; Heppner & Maynard 1983, 1987; Heelis *et al.* 1982) have been designed specifically to retain the sharp boundaries which are a feature of many of the observations. This mismatch in representation creates problems when trying to understand the effects of precipitation for given convection conditions. In particular, it may require recognition of the fact that, under some conditions, existing precipitation models are totally inappropriate. Further difficulties in attempting to evaluate quantitatively the interaction of convection and precipitation are caused by the lack of data giving the B_y dependence of the precipitation patterns, and there is little information on the evolution of precipitation patterns under time-varying convection conditions (this is discussed further in §3). It is only in rare cases that good precipitation and convection data are simultaneously available. This lack of the required data poses a significant problem when trying to understand the interaction of convection and precipitation, and the ionospheric consequences, particularly on the nightside.

To illustrate this point, we present the results of electron density calculations corresponding to the EISCAT observations shown in figure 3 and based on the model convection velocities shown in figure 4. Figure 6 shows observed values of electron density from gate 3 (*ca.* 277 km, near the F2-peak) and calculated values for this day. The modelled data are shown for two levels of particle precipitation based on the Spiro *et al.* (1982) statistical models taken from *Atmosphere Explorer* satellite data. The precipitation patterns used were radially scaled in order to match the polar cap boundary of the convection pattern with the latitude of the peak energy flux in the precipitation.

In the later part of the observations, where convection conditions have become established, quite good agreement between observed and calculated values is achieved, even to the extent of producing the double peak structure observed by EISCAT. It is significant that the agreement improves near dawn as photoionization becomes more important than precipitation (though the duskside behaviour, where agreement is also good, is the consequence of both photoionization and precipitation).

In the early part of the observations, where convection conditions in the previous period are unknown (but there is some evidence for a preceding disturbed period), calculations do not match well with observations. These nightside calculations are sensitive to the assumed precipitation model, and we have no data to indicate which model is appropriate to the observations. On the dayside and in the afternoon the predominance of photoionization removes such sensitivity.

PHILOSOPHICAL TRANSACTIONS OF THE ROYAL SOCIETY A MATHEMATICAL, PHYSICAL & ENGINEERING SCIENCES

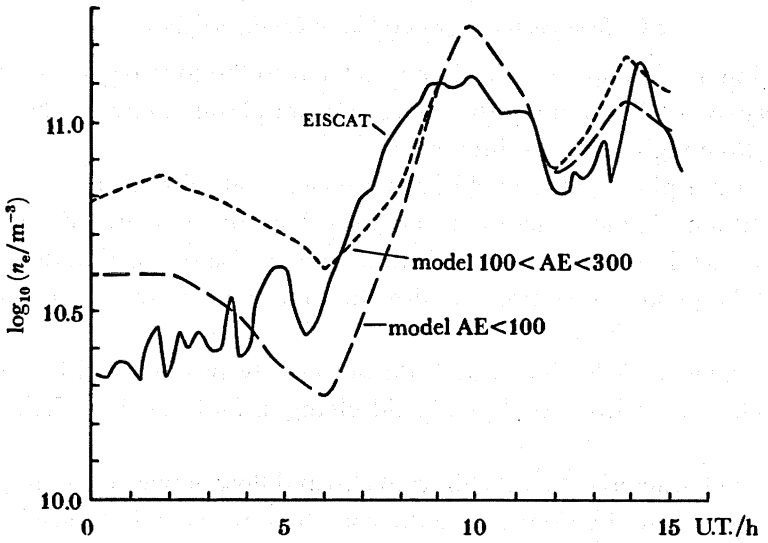

FIGURE 6. Observed and calculated electron concentrations corresponding to gate 3 (at an altitude of 277 km) of the observations shown in figure 3.

2.5. *Ionosphere–thermosphere interactions*

At high latitudes, plasma convection provides a major source of momentum and energy for the neutral atmosphere by collisional interactions, giving ion drag and heating both of the ions and neutral gases. As a result, thermospheric circulation at high latitudes is dominated not by solar heating generated pressure gradients but by direct ion drag and heating in the auroral oval, as well as by the Coriolis force. The linkage between the neutral and ionized gases is highly dependent on electron densities and on the stability of the overall convection pattern. As the timescale for the response of the neutral atmosphere to a new set of convection conditions is of the order of 1 h or greater, time-varying convection can lead to the wind being unable to respond to the ion motions, with consequent heating and effects on the chemical decay of plasma (see §2.3).

Convection driven large antisunward winds play a crucial role in the maintenance of the nightside high-latitude F-layer, particularly in the trough region in the post-midnight sector. Here, convection-driven winds act as a momentum source to raise the altitude of the F-layer, (see §2.1), to regions of lower neutral gas densities and hence lower decay rate, and as a result significantly increasing the lifetime of the ionospheric plasma. Without the large wind velocities caused by convection, the ionosphere in this region would collapse. As an example, for the calculations shown in figure 6, setting the neutral wind to zero reduced the calculated altitude of the F2-peak in the early morning from *ca.* 300 km to *ca.* 260 km, and calculated electron concentration values at 277 km were reduced from 4.0×10^{10} to 1.1×10^{10} m^{-3}. The calculations carried out by Quegan *et al.* (1982) show an even more drastic collapse of the ionosphere in the absence of winds. Note that at lower latitudes large winds are not necessary to maintain the nightside ionosphere, because the protonosphere acts as a production source for the F-layer. Downflowing H^+ charge exchanges with neutral O to provide an O^+ source.

PHILOSOPHICAL TRANSACTIONS OF THE ROYAL SOCIETY A MATHEMATICAL, PHYSICAL & ENGINEERING SCIENCES

2.6. *Ionosphere/magnetosphere field-aligned flows*

Plasma convection at high latitudes is directly related to the topology of the magnetic field, which in turn is crucial in determining the interchange of plasma between the ionosphere and magnetosphere. Three régimes are of interest:

(1) the inner plasmasphere, where field lines are closed at all times;

(2) the high-latitude régime, where plasma is involved in the convection cycle, and field lines are open for a certain proportion of their time, the precise proportion depending on their travel time across the polar cap compared with the time spent in the return flow part of the cycle;

(3) a boundary layer of field lines which do not clearly belong to either of the first two régimes, and which are sensitive to electric field changes, and possibly U.T. (Quegan *et al.* 1986).

The first régime is characterized by the diurnal ebb and flow of plasma, acting as a nighttime source of plasma to stabilize the F-layer (see the comment at the end of the §2.5). The second régime is subject to polar wind outflow and wave-induced events by which heavy ions can be ejected from the ionosphere. The third régime is less easily characterized, and is highly affected by the time between openings of the field lines and by meridional drifts caused by the convection electric field. Such drifts, if they have the right phasing, can act like pumps, sucking plasma up in the day as the plasma moves to higher latitudes and flux-tubes increase in volume, and then squeezing it down at night as it retreats to lower latitudes, and can greatly accelerate the refilling process described by Park (1974) and Murphy *et al.* (1976).

The ionospheric consequences of field-aligned flows at high latitudes are closely related to convection, because outflow of plasma is a slowly acting loss term (of the order of hours) for ionospheric plasma, which only leaves its mark if plasma is not exposed to production sources for an extended period of time. As a result, the effects of plasma outflows are dependent on the plasma trajectories in the convection pattern. Only on some convection paths will significant effects develop. In particular, plasma following convection paths such as path 5 in figure 1 spends many hours in darkness and away from production sources, and will be significantly affected by plasma outflows. It is on such convection paths that the mid-latitude trough is formed, and plasma outflow contributes significantly to the formation and characteristics of the morningside trough.

A related topic is the occurrence of deep holes of ionization in the polar cap. Brinton *et al.* (1978) describe a particularly long-lived example, but they are found in profusion in *Ariel*-4 data, and elsewhere (A. S. Rodger, personal communication). Such features can be understood in terms of convection, as regions of plasma stagnating or trapped in a vortex away from sunlight or any other production source, and have been successfully modelled from this point of view. However, it is not all clear what the flow signature above such a localized decaying feature should be. Downflows may be possible.

2.7. *Universal Time effects*

Considerable complexity is added to our description of the high-latitude ionosphere because of the offset of the geographic and geomagnetic poles, with particularly large effects occurring in the Southern Hemisphere. The frame within which we describe plasma convection makes a large difference to the simplicity of that description (see figure 5). Moreover, because

PHILOSOPHICAL TRANSACTIONS OF THE ROYAL SOCIETY A MATHEMATICAL, PHYSICAL & ENGINEERING SCIENCES

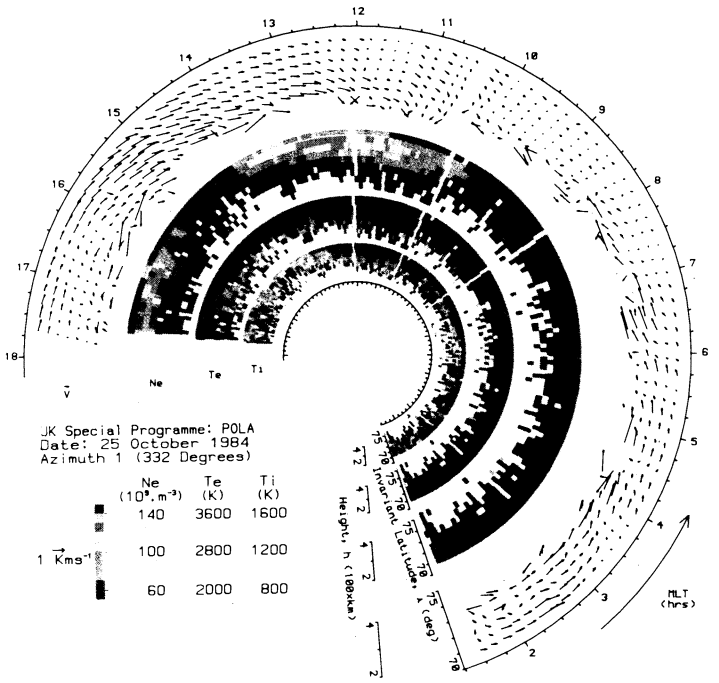

FIGURE 3. Polar dial plot of EISCAT data from the U.K. Special Programme, Polar, for 25 October 1984 on azimuth 1 (332°). It consists of concentric plots of invariant latitude against MLT with 10 min averages of velocity vectors, $\boldsymbol{V}$, plasma density, N, electron and ion temperatures, T_e and T_i.

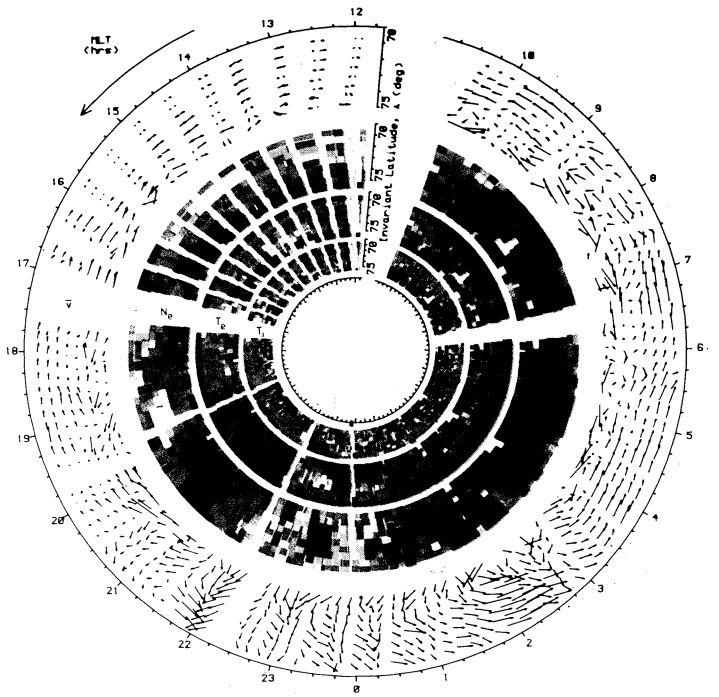

FIGURE 8. Similar to figure 7, but for the situation shown in figure 6*c* (Killeen *et al.* 1988); day 340, 1981, orbit 1849. K_p is 2^-; the IMF is $\boldsymbol{B} = (-4.0, +4.0, -2.5)$.

(*Facing p.* 130)

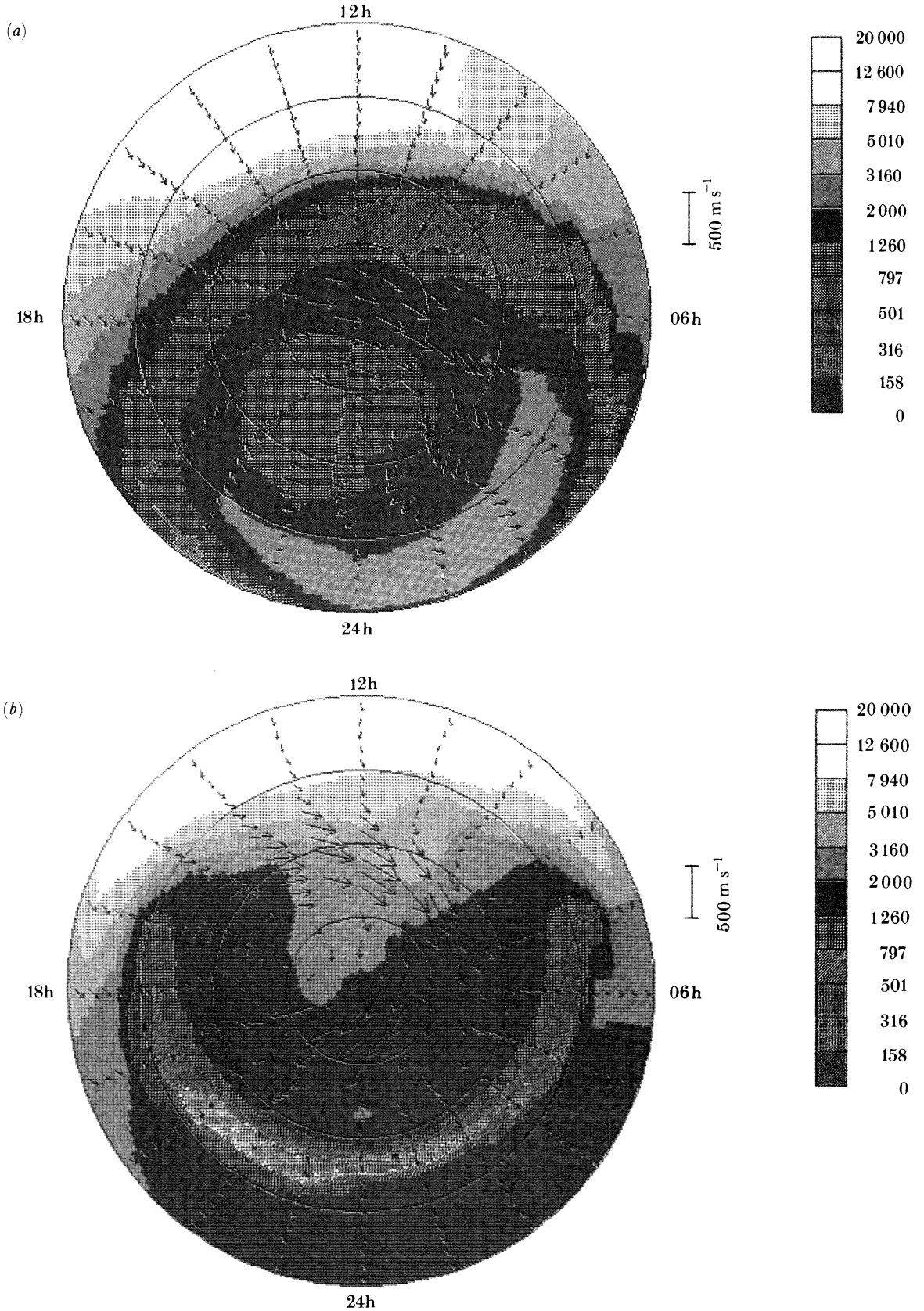

FIGURE 7. Calculated electron concentrations (in units of 10^8 m^{-3}) at pressure level 12 (near 300 km), 50–90° latitude, from the coupled UCL–Sheffield thermosphere–ionosphere model, at (*a*) 06h and (*b*) 18h U.T. The calculations are carried out by using the BC–DE electric field models of Heppner & Maynard (1987) for the Northern Hemisphere on 21 December with $F_{10.7}$ = 185, *Tiros* activity level 7 augmented by DMSP data at low energies. The arrows on the figure are wind vectors.

photoionization is under geographic control while convection and precipitation show organization in the geomagnetic frame, large physical effects are associated with the need to consider both frames.

Understanding thermospheric winds and ionospheric structures relies heavily on the diurnal oscillation of the convection pattern about the geographic pole (Hays *et al.* 1984; Fuller-Rowell *et al.* 1987). Figure 7, plate 2, shows a plot of calculated electron densities near the F2-peak at 06h00 and 18h00 U.T. for the Northern Hemisphere at the winter solstice, using the UCL–Sheffield coupled thermosphere–ionosphere model under moderate solar and geomagnetic activity for an $F_{10.7}$ (solar radio flux) value of 185×10^{-22} W m^{-2} Hz^{-1} and B_y positive conditions (UCL is University College London). Also marked are the calculated thermospheric wind vectors, but these are not discussed here (see Rees *et al.* 1987).

At 06h00 U.T. the convection pattern is at its most antisunward. Because of the lack of photoionization, the auroral oval stands out as a region of enhanced electron density, though the enhancement is not great (see the contour levels). Because the calculations are carried out for the winter solstice and the convection pattern is of limited extent, no portion of the convection pattern enters sunlight at this time. As a result, plasma convecting from the morning-side continues to decay even into the noon sector, giving a dayside mid-latitude trough; the mid-latitude trough encircles the polar region. An important feature of this figure is the region of enhanced electron densities in the post-midnight sector, because it shows how necessary it is to consider timescales and the history of the plasma when interpreting observations or (in this case) simulations. This enhancement is not as a result of precipitation, though precipitation contributes; it is, in fact, a remnant of plasma convected from the dayside under earlier sunlit conditions.

At 18h00 U.T., the convection pattern is at its furthest sunward location. Because the convection cells extend into sunlight, they are able to transport plasma from the dayside into the polar cap, spreading plasma over the northern high-latitude region. The auroral oval no longer stands out, and the asymmetry of the electron density distribution at 06h00 U.T. is no longer noted. The mid-latitude trough is now confined to the nightside, and its deepest values occur in the pre-midnight and midnight sectors; this asymmetry is again a symptom of plasma at different points having had different times since they were last exposed to ionization sources.

3. The role of convection in understanding observations

Section 1 has shown that convection is deeply embedded in the major processes determining the behaviour of the high-latitude ionosphere. A number of examples have shown how convection is essential in understanding observations, in combination with a consideration of timescales of processes and of past history. We now cite two widely contrasting examples dealing with topics barely mentioned above, as a furter confirmation of the need to consider convection in understanding almost any ionospheric measurements at high latitudes.

3.1. *The topside ionosphere: regions of* He^+ *dominance*

Most of the examples quoted above have dealt with F-layer phenomena. The following example is chosen to illustrate the importance of convection to the topside ionosphere, and also because of its relevance to results in the paper by Moffett *et al.* in this Symposium.

At most times plasma in the topside ionosphere has O^+ or H^+ as the dominant ion. However, observations of He^+ dominance in the topside high-latitude ionosphere have been noted by Hoffman *et al.* (1974), Shepherd *et al.* (1976) and Heelis *et al.* (1981). A study by Quegan *et al.* (1984) has carefully analysed conditions under which such phenomena can be caused. Their principal conclusion was that He^+ dominance was caused by transport of depleted plasma through a region where the topside was illuminated, giving production of He^+, while the lower ionosphere was not illuminated, giving little production of O^+ (and hence H^+). Crucial to this explanation is convection, its relation to production sources, and its occurrence at high latitudes. Firstly, convection at high latitudes causes plasma decay by transport of plasma into regions of no production sources, in the absence of the protonospheric reservoir available at mid-latitudes. This creates the initial depletion. Secondly, transport back towards sunlight into regions where only the upper atmosphere is illuminated gives the conditions for a build-up of He^+, without significant enhancement of O^+ or H^+. Transit through régimes satisfying these solar zenith angle conditions should not be too fast, so that He^+ has time to build up, and hence convection conditions are critical to the generation of such He^+ dominant regions. It is of considerable interest to compare these conclusions with those contained in the accompanying paper by Moffett *et al.*; totally different mechanisms come into play at mid-latitudes.

3.2. *Time-varying convection conditions*

As a marked contrast to the last example, where observations were explained in terms of the general properties of convection, in particular transport from plasma decay regions into regions of decreasing solar zenith angle, the second example relates to specific conditions on a particular day when EISCAT and Sondre Stromfjord simultaneous incoherent scatter radar observations allowed strong inferences to be made about the time-dependent behaviour of the convection electric field.

Observations made on 3–4 February 1984 by EISCAT have been described by Lockwood *et al.* (1986). They exhibit dramatic time-dependent behaviour which was simultaneously observed by the incoherent scatter facility at Sondre Stromfjord, and by the *Dynamics Explorer* 1 satellite (*DE* 1). This permitted an unusually well-documented description of the convection electric field to be formulated. Unfortunately, energetic charged-particle data for this same period were not available.

Figure 8, plate 1, is a dial plot of the EISCAT observations for this period. The velocity vectors prior to 22h00 MLT show the signature of a dusk cell, with westward flow predominating. Flows at the highest latitudes appear irregular; this may be caused by poor signal-to-noise ratios, since the electron densities at these latitudes are low at all times. There is no clear systematic latitudinal variation in the magnitude of the zonal velocities. The period from 20h00 to 22h00 MLT shows outflow from the polar cap and the Harang discontinuity, with the flows turning to westwards at the later MLTs. At 22h00 there is a sharp change in the convection pattern, as westward and equatorward flows suddenly occur, followed by a period of marked equatorward flow, turning eastward as time increases.

The electron densities show a midday peak, with a decline to low values near 17h00 MLT. An increase near dusk is followed by a marked depression near 21h00 MLT. At around 21h30, values begin to increase, reaching their maximum near magnetic midnight, then falling to low values in the whole of the morning sector. The values observed in the midnight sector exceed the noon-time values.

PHILOSOPHICAL TRANSACTIONS OF THE ROYAL SOCIETY A MATHEMATICAL, PHYSICAL & ENGINEERING SCIENCES

Lockwood *et al.* (1986) interpreted these observations, with the addition of Sondre Stromfjord and *DE* 1 data, as indicating a massive increase in the cross-tail potential difference (by 200 kV !) with subsequent expansion of the polar cap. The observations at EISCAT correspond to the passage of the polar cap boundary across the field of view as the cap expands. The increase in potential difference occurred at around 19h20 U.T. and the polar cap expansion continued until around 20h16 U.T. Conditions then remained steady for a period of *ca.* 4 h, before the polar cap deflated again.

This event has been modelled by using a convection electric field from Heelis *et al.* (1982), because of the simplicity with which the field can be parametrized. A symmetrical two-celled pattern was adopted, with the separatrix of the two cells being inclined at 15° to the noon–midnight meridian, i.e., aligned along the 11h00–23h00 MLT meridian. The convection pattern was centred on a point displaced 3° towards midnight from the magnetic pole, as deduced by Lockwood *et al.* (1986). The values for the cross-tail potential difference used were 60 kV before 19h20 U.T. and after 00h16 U.T. and 260 kV in the period 19h20–00h16 U.T. The polar cap radius was taken as 12.5° at 19h20 U.T., increasing linearly with time to 21° at 20h16 U.T.; this value was sustained until 00h16, after which it returned to its initial value linearly with time over a period of 1 h. These parameters gave reasonable agreement between observed and modelled convection data. A fuller discussion is given in Quegan *et al.* (1988).

To model the electron density behaviour, the following parameters were adopted. The neutral atmosphere was taken from the MSIS-83 (mass spectrometer and incoherent scatter) model (Hedin 1983) for the appropriate day of the year, with $A_p = 1.0$, $AE = 310.0$, and an $F_{10.7}$ value of 120×10^{-22} W m^{-2} Hz^{-1}. The precipitation data were from the *Tiros*–DMSP data-set (Fuller-Rowell & Evans 1987), scaled from activity level 3 to 9 on the same timescales as for the polar cap radius (*Tiros* is the television and infrared observations satellite, DMSP is the Defense Meteorological Satellite Program). No matching of precipitation to convection boundaries has explicitly been carried out, and hence the results presented constitute only a first attempt at modelling. The neutral wind data used were identical to those adopted by Quegan & Gill (1987). Calculations were carried out for the position of EISCAT gate 3 in the Polar programme.

The electron densities corresponding to gate 3 of the observations were calculated by using the procedures described by Quegan & Gill (1987). The results are shown in figure 9. They show good agreement with figure 8 from dusk onwards as we now make clear. The duskside peak in electron density followed by a decline to very low values near 20h30 MLT is well reproduced. This is followed by increasing values, with a sharp increase near 22h30, which again corresponds to the observations. Densities stay high until midnight, peak values occurring just before this time. After midnight there is a rapid decrease in electron density; this occurs in the observations, but *ca.* 1 h later. The morning sector densities are low in the observations; in the calculations the values are comparable with values for the evening sector. However, no proper comparison is possible without access to the quantitative values associated with the colour coding of figure 8.

The calculated electron densities before dusk do not closely represent the features in the observations. The noon and afternoon peak in electron density is reproduced, with values slightly higher than the calculated midnight values (in the observations, the higher values occur near midnight). These values decline slowly, and the dip in ionization present in the observations near 17h00 MLT is not reproduced in the calculations. As shown by Quegan *et al.*

PHILOSOPHICAL TRANSACTIONS OF THE ROYAL SOCIETY A MATHEMATICAL, PHYSICAL & ENGINEERING SCIENCES

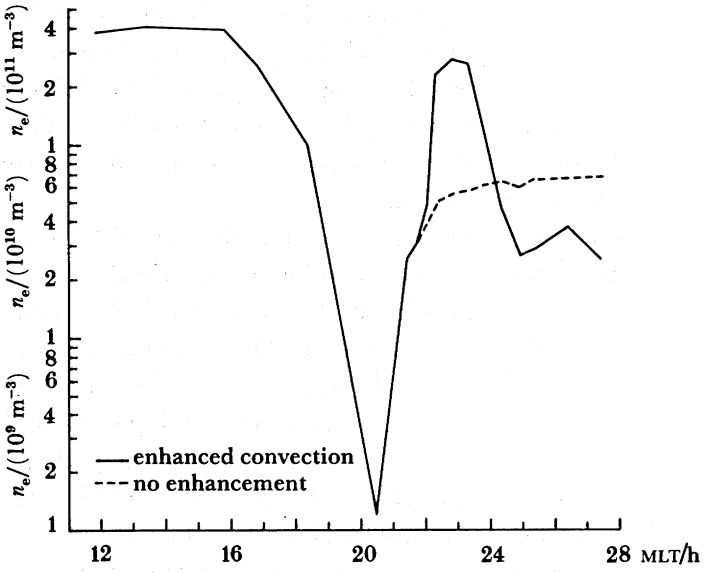

FIGURE 9. Calculated electron concentrations at gate 3 for the conditions of the observations in figure 8. The dashed curve beginning near 21h00 MLT corresponds to calculations without a convection enhancement.

(1988), this trough feature depends on the proper location of the dusk cell, since it is caused by plasma between ionization (photon and particle) sources, which may have travelled well into the nightside. Incorrect location of this cell and the associated precipitation regions would affect any attempt at reproducing this feature.

Also marked on figure 9 are the calculated electron densities in the absence of the convection enhancement. There are two notable features. Firstly, the convection enhancement has a marked effect on the calculated values *ca.* 40 min after the enhancement begins, giving an approximately five-fold relative increase in electron density. Secondly, the morning values are significantly reduced when the convection enhancement occurs, compared with when it does not. The low morning values of the observations are quite notable, and the calculations appear to reproduce this trend. Analysis of the calculations shows that the low morning electron densities are caused by plasma following long convection paths in darkness. This conclusion should be treated with caution, however, because of the uncertainties in precipitation boundaries.

4. CONCLUSIONS

Plasma convection is deeply embedded in the structure of the high-latitude ionosphere, influencing in some way almost every major process affecting plasma densities. Understanding observations requires us to take these convection effects into consideration. When we observe plasma we must remember that the plasma we see has arrived from elsewhere; along the way it has been exposed to numerous processes having differing timescales, many of which are greatly affected by the convection process itself. Proper understanding of the data needs us to recognize the processes, the relevant timescales, the interaction of processes and their mutual consistency. Only if we do all that can we 'understand' the data and arrive at a correct interpretation of the observations. This is a major argument for large-scale models, but carries

PHILOSOPHICAL TRANSACTIONS OF THE ROYAL SOCIETY A MATHEMATICAL, PHYSICAL & ENGINEERING SCIENCES

with it the problem of describing self-consistently the inputs needed to arrive at realistic physical predictions.

When reasonable estimates of the convection electric field are available, model calculations seem capable of reproducing the characteristics of observed plasma behaviour. A continual difficulty with such calculations, particularly on the nightside, is that of describing the particle precipitation input in a way consistent with the convection conditions. The thermospheric wind, which is an important determinant of the nightside ionosphere particularly at trough latitudes, can be determined self-consistently with a convecting ionosphere, at a significant computing cost. The question of field-aligned flows above a convection-induced stagnation feature remains open.

In many cases, good estimates of the convection electric field are not available from direct observation, and they must be inferred from solar wind parameters. Recent work offers hope that this may lead to viable methods (Etemadi *et al.* 1989; Lockwood, this Symposium); the problem of providing consistent precipitation signatures still remains.

Recent work at Rice University (R.W. Spiro, personal communication) is also likely to lead to an understanding of the latitudinally narrow belts of enhanced convection observed at subauroral latitudes (Spiro *et al.* 1979), and of their ionospheric consequences. This will in turn shed light on high-latitude troughs, and their relation to convection, to provide yet another example of how understanding the high-latitude ionosphere and understanding convection go hand in hand.

I would like to express my gratitude for being permitted to use EISCAT data (EISCAT is supported by the British SERC, French CNRS, West German MPG, Norwegian NAVF, Swedish NFR and Finnish SA), and particularly to M. Lockwood for useful discussions relating to them. I also thank Marconi Research Centre for permission to use figure 9, which is taken from a Marconi Technical Report.

REFERENCES

Brinton, H. C., Grebowsky, J. M. & Brace, L. H. 1978 *J. geophys. Res.* **83**, 4767–4776.
Cowley, S. W. H. 1981*a* *Planet. Space Sci.* **29**, 79–96.
Cowley, S. W. H. 1981*b* *Planet. Space Sci.* **29**, 809–818.
Dungey, J. W. 1961 *Phys. Rev. Lett.* **6**, 47–48.
Etemadi, A., Cowley, S. W. H. & Lockwood, M. 1989 *J. atmos. terr. Phys.* (In the press.)
Evans, J. V., Holt, J. M., Oliver, W. L. & Wand, R. H. 1983 *J. geophys. Res.* **88**, 7769–7782.
Fuller-Rowell, T. J. & Evans, D. S. 1987 *J. geophys. Res.* **92**, 7606–7618.
Fuller-Rowell, T. J., Rees, D., Quegan, S., Moffett, R. J & Bailey, G. J. 1987 *J. geophys. Res.* **92**, 7744–7748.
Grebowsky, J. M., Taylor, H A. Jr & Lindsay, J. M. 1983 *Planet. Space Sci.* **31**, 99–105.
Hays, P. B., Killeen, T. L., Spencer, N. W., Wharton, L. E., Roble, R. G., Emery, B. A., Fuller-Rowell, T, J., Rees, D., Frank, L. A. & Craven, J. D. 1984 *J. geophys. Res.* **89**, 5597–5612.
Hedin, A. E., 1983 *J. geophys. Res.* **88**, 10170–10188.
Heelis, R. A., Lowell, J. K. & Spiro, R. W. 1982 *J. geophys. Res.* **87**, 6339–6345.
Heelis, R. A., Murphy, J. A. & Hanson, W. B. 1981 *J. geophys. Res.* **86**, 59–64.
Heelis, R. A. & Reiff, P. H. 1985 *Adv. Space Res.* **5** (4), 349–362.
Heelis, R. A., Winningham, J. D., Hanson, W. B. & Burch, J. L. 1980 *J. geophys. Res.* **85**, 3315–3324.
Heppner, J. P. 1977 *J. geophys Res.* **82**, 1115–1125.
Heppner, J. P. & Maynard, N. C, 1983 *Proc. Chapman Conf., Irvington, Virginia.*
Heppner, J. P. & Maynard, N. C. 1987 *J. geophys. Res.* **92**, 4467–4489.
Hill, T. W. 1983 Solar-wind–magnetosphere coupling. In *Solar-Terrestrial Physics* (ed. R. L. Carovillano & J. M. Forbes), p. 261. Hingham, Massachusetts: Reidel.
Hoffman, J. H., Dodson, W. H., Lippincott, C. R. & Hammack, H. D. 1974 *J. geophys. Res.* **79**, 4246–4251.
Lockwood, M., van Eyken, A. P., Bromage, B. J. J., Waite, J. H. Jr., Moore, T. E. & Doupnik, J. R. 1986 *Adv. Space Res.* **6** (3), 93–101.

Moore, T. E., Lockwood, M., Chandler, M. O., Waite, J. H. Jr, Chappell, C. R., Persoon, A. & Sugiura, M. 1986 *J. geophys Res.* **91**, 7019–7031.
Mozer, F. S. 1984 *Geophys. Res. Lett.* **11**, 135–138.
Murphy, J. A., Bailey, G. J. & Moffett, R. J. 1976 *J. atmos. terr. Phys.* **38**, 351–364.
Park, C. G. 1974 *J. geophys. Res.* **79**, 169.
Pinnock, M. 1985 *J. atmos. terr. Phys.* **47**, 1111–1121.
Quegan, S., Bailey, G. J. & Moffett, R. J. 1984 *Planet. Space Sci.* **32**, 791–802.
Quegan, S., Bailey, G. J., Moffett, R. J., Heelis, R. A., Fuller-Rowell, T. J., Rees, D. & Spiro, R. W. 1982 *J. atmos. terr. Phys.* **44**, 619–640.
Quegan, S., Bailey, G. J., Moffett, R. J. & Wilkinson, L. C. 1986 *J. atmos. terr. Phys.* **48**, 25–40.
Quegan, S. & Gill, R. S. 1987 *Marconi Tech. Rep.* MTR 87/6.
Quegan, S., Gill, R. S., & Lockwood, M. 1988 *J. atmos. terr. Phys.* **50**, 1057–1076.
Rees, D., Fuller-Rowell, T. J., Quegan, S., Moffett, R. J. & Bailey, G. J. 1987 *Annls Geophysicae* A **5**, 303–328.
Reiff, P. H. 1982 *J. geophys. Res.* **87**, 5976–5980.
Reiff, P. H., Spiro, R. W. & Hill, T. W. 1981 *J. geophys. Res.* **86**, 7639–7648.
Rezhenov, B. V. 1981 *Planet. Space Sci.* **29**, 687–693.
Rino, C. L. & Vickrey, J. F. 1982 *J. atmos. terr. Phys.* **44**, 875–887.
Rodger, A. S., Brace, L. H., Hoegy, W. R. & Winningham, J. R. 1986 *J. atmos. terr. Phys.* **48**, 715–728.
St Maurice, J. P. & Torr, D. G. 1978 *J. geophys. res.* **83**, 969–977.
Schunk, R. W. 1975 *Planet. Space Sci.* **23**, 437–485.
Shepherd, G. G., Whitteker, J. H., Winningham, J. C., Hoffman, J. H., Maier, E. J., Brace, L. H., Burrows, J. R. & Cogger, L. L. 1976 *J. geophys. Res.* **81**, 6092–6102.
Sojka, J. J., Foster, J. C., Raitt, W. J., Schunk, R. W. & Doupnik, J. R. 1980 *J. geophys. Res.* **85**, 703–709.
Sojka, J. J. & Schunk, R. W. 1986 *J. geophys. Res.* **91**, 259–269.
Spiro, R. W., Heelis, R. A. & Hanson, W. B. 1979 *Geophys. Res. Lett.* **6**, 657–660.
Spiro, R. W., Reiff, P. H. & Maher, L. J. Jr 1982 *J. geophys. Res.* **87**, 8215–8227.
Volland, H. 1975 *Annls Geophys.* **31**, 159–174.
Zanetti, L. J., Potemra, J. A., Iijima, T., Baumjohann, W. & Bythrow, P. F. 1984 *J. geophys. Res.* **89**, 7453–7458.

Discussion

A. S. Rodger (*British Antarctic Survey, Cambridge, U.K.*). The formation processes for the main (or mid-) latitude trough and high-latitude trough can be rather different and thus they should really be considered separately. In Dr Quegan's simple example he showed parcels of plasma travelling across the terminator from the dayside into the nightside. This is not the normal flow direction in the main ionospheric trough when the flow is towards the dayside and thus this model is only appropriate in considering high-latitude trough formation.

Under steady-state and relatively quiet geomagnetic conditons, the 'stagnation' of plasma is of major importance in the formation of the main ionospheric trough. Under more active conditions, when large electric fields associated with subauroral ion-drift events are present, the enhanced recombination process, suggested by St Maurice, Schunk and others, must become important. His modelling work will be very valuable in assessing the relative importance of the two processes in trough formation. This might be expected to vary as a function of geomagnetic activity, U.T., season, ion drift speed, etc.

There are likely to be a variety of mechanisms that could be responsible for the formation of high-latitude troughs. For example, they can occur on flux tubes which do not convect into sunlight or into regions of energetic particle precipitation for an extended period. Also troughs may occur in regions of heating where field-aligned plasma flow will be the dominant process. Each of these mechanisms for high-latitude trough formation will have a rather distinctive signature in terms of parameters such as electron and ion temperatures, horizontal and vertical plasma motions, etc. Thus experiments such as incoherent scatter radars will be invaluable for providing the necessary input parameters for his model calculations.

PHILOSOPHICAL TRANSACTIONS OF THE ROYAL SOCIETY A MATHEMATICAL, PHYSICAL & ENGINEERING SCIENCES

S. Quegan. The little example given in the paper was not really intended to be realistic; it does illustrate, however, that one must beware of simplistic reasoning about trough formation under fast convection, and that was its purpose.

I agree wholeheartedly that our understanding of high-latitude troughs, and troughs associated with fast convection, is incomplete. The relative importance of a number of depletion mechanisms needs to be clarified. Part of the problem in carrying out a proper investigation of these phenomena is that one requires consistent treatment of a variety of processes, typically in a time-dependent situation. As a result, no proper investigation has yet been performed.

P. J. S. Williams (*Coleg Prifysgol Cymru, Aberystwyth, U.K.*). 1. On occasions we observe, with EISCAT, short-lived but very powerful plasma fluxes upward along the field line, with velocities as high as 1 km s^{-1}. Events like these are a major factor in the formation of high-latitude holes and troughs.

2. Following this I would like to stress the effect which O–O^+ collisions have on diffusion, ion drag, and upward acceleration. The value of the collision cross section is still in dispute, with values over a range of 5:1 being quoted. Models will be sensitive to value adopted.

S. Quegan. 1. To evaluate the significance of such flows as a means of forming high-latitude structures, one needs to look carefully at the duration of the flows and the timescales of the depletion process. Short transients are likely to have little consequence for electron densities.

2. This is a longstanding bone of contention. There is considerable disagreement among investigators as to whether currently adopted values for the O^+–O collision frequency are too high, too low or correct. As a result, the only meaningful studies which can be carried out at the moment treat the O^+–O collision frequency as a variable parameter; such a study is under discussion at UCL and Sheffield.

M. Lockwood (*Rutherford Appleton Laboratory, Didcot, U.K.*). The large upflows are ultimately driven by large, probably transient, electric fields via the effects of collisions with the neutral thermosphere giving expansion due to Joule heating, ion–neutral frictional heating and an upwards force because the ion velocity distribution becomes anisotropic in an inhomogeneous magnetic field. The upflows must be transient because the ionosphere could not sustain such large fluxes for more than *ca.* 10 min. However, what is transient for one flux tube can be continuous if flux tubes are convected through the region of plasma heating sufficiently quickly.

H. Rishbeth (*University of Southampton, U.K.*). In calculating the vertical drifts due to electric fields, it is essential to take careful account of the neutral air motion. Under conditions of high ion density and strong ion drag, the plasma and air motions are horizontal; there is no vertical drift. More generally, the Coriolis force and inertia will affect the wind speed and direction, and hence affect the local time and U.T. variation of the drift.

In a Symposium dedicated to Sydney Chapman, we might recall that the theory of ionospheric electrodynamics owes much to another great guru, D. F. Martyn.

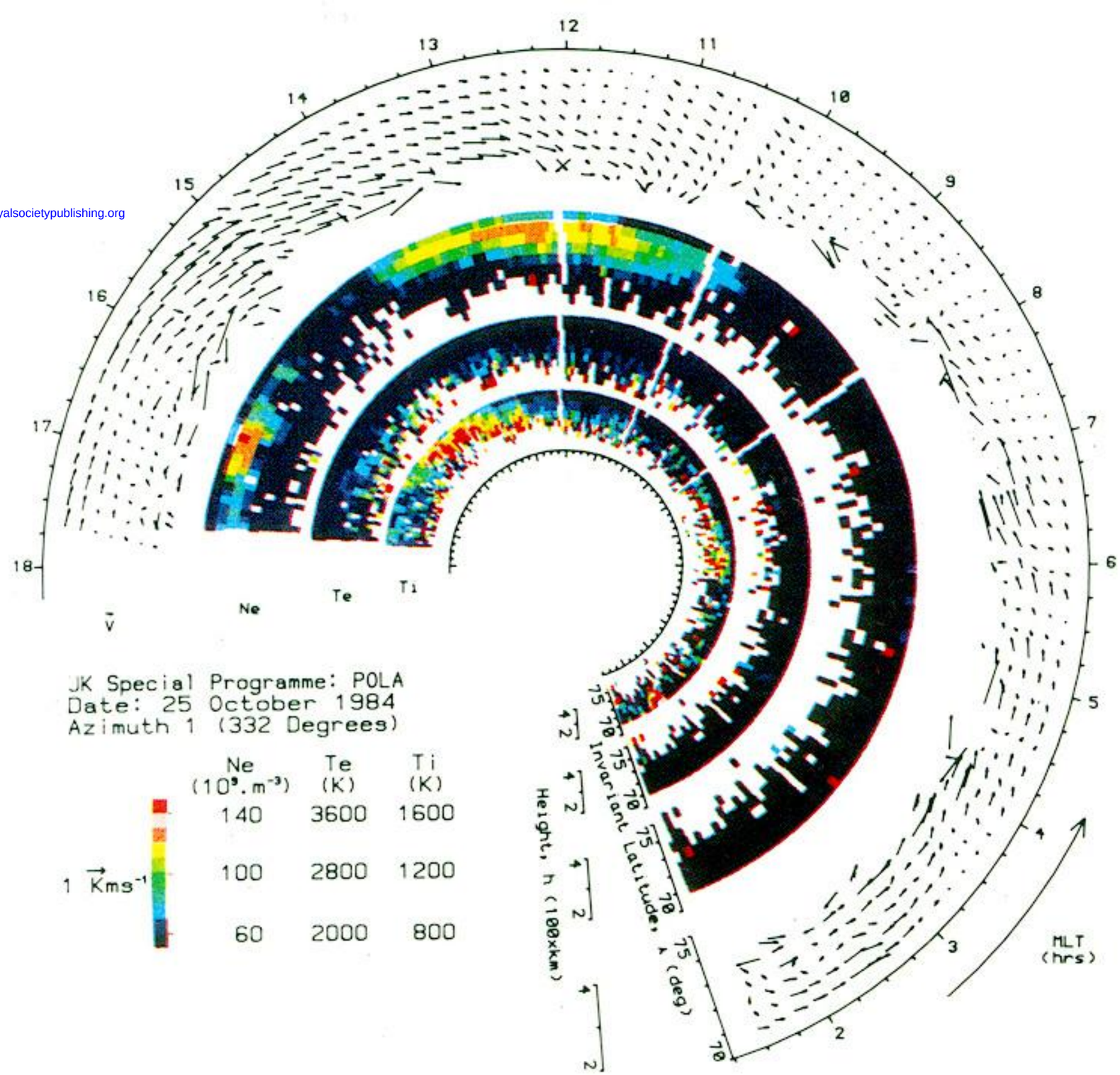

FIGURE 3. Polar dial plot of EISCAT data from the U.K. Special Programme, Polar, for 25 October 1984 on azimuth 1 (332°). It consists of concentric plots of invariant latitude against MLT with 10 min averages of velocity vectors, $\boldsymbol{V}$, plasma density, N, electron and ion temperatures, T_e and T_i.

PHILOSOPHICAL TRANSACTIONS OF THE ROYAL SOCIETY A MATHEMATICAL, PHYSICAL & ENGINEERING SCIENCES
PHILOSOPHICAL TRANSACTIONS OF THE ROYAL SOCIETY A MATHEMATICAL, PHYSICAL & ENGINEERING SCIENCES

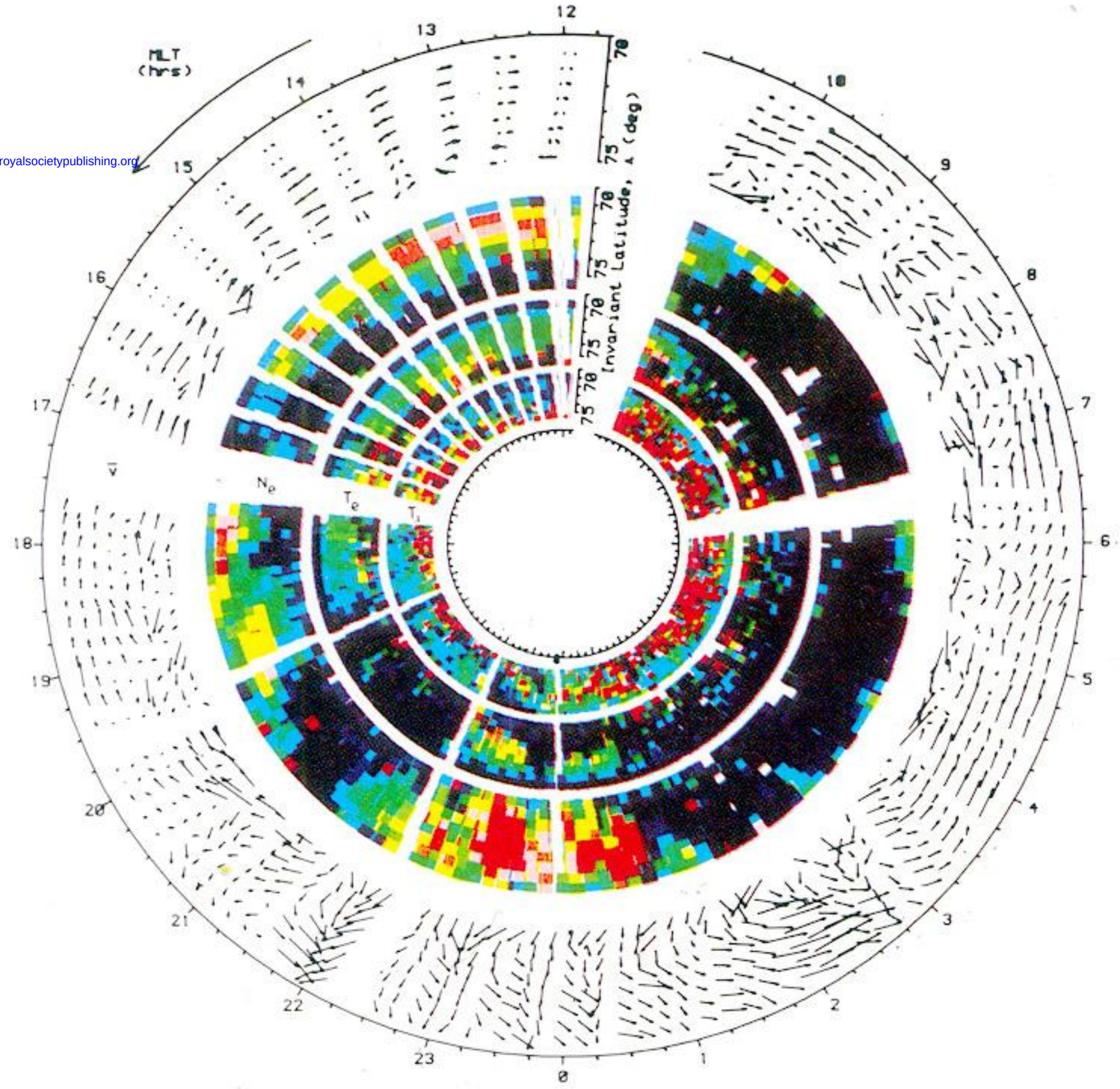

IGURE 8. Similar to figure 7, but for the situation shown in figure 6*c* (Killeen *et al.* 1988); day 340, 1981, orbit 1849. K_p is 2^-; the IMF is $\boldsymbol{B} = (-4.0, +4.0, -2.5)$.

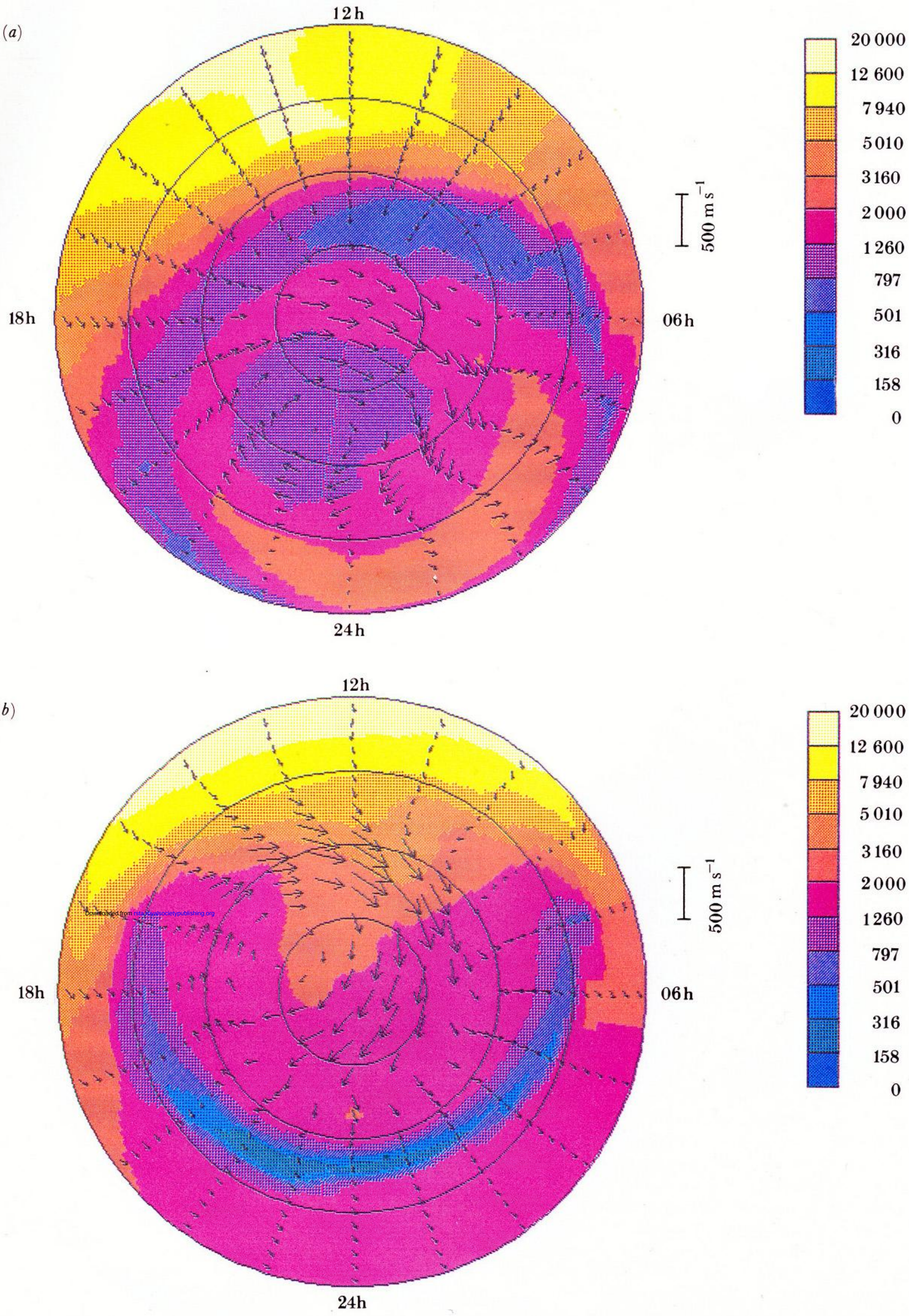

FIGURE 7. Calculated electron concentrations (in units of 10^8 m^{-3}) at pressure level 12 (near 300 km), 50–90° latitude, from the coupled UCL–Sheffield thermosphere–ionosphere model, at (*a*) 06h and (*b*) 18h U.T. The calculations are carried out by using the BC–DE electric field models of Heppner & Maynard (1987) for the Northern Hemisphere on 21 December with $F_{10.7}$ = 185, *Tiros* activity level 7 augmented by DMSP data at low energies. The arrows on the figure are wind vectors.